High-Temperature Oxidation of CVD β-SiC Part I. Experimental Study

J. Rodríguez-Viejo,[a] F. Sibieude[b] & M. T. Clavaguera-Mora[a]

[a] Grupo de Física de Materiales, Depto de Física, Facultad de Ciencias, Universidad Autónoma de Barcelona, 08193 Bellaterra, Spain

[b] Institut de Sciences et de Génie des Matériaux et Procédés, C.N.R.S. Odeillo, 66120 Font Romeu, BP5, France

(Received 12 May 1993; accepted 15 October 1993)

Abstract

The oxidation kinetics of β-SiC prepared by chemical vapor deposition (CVD) in dry oxygen (3×10^{-2}–80 atm) was investigated over the temperature range 1200 to 1550°C.

In situ *X-ray diffraction was used to measure the silica layer thickness at $P_{O_2} \leq 1$ atm. At higher pressures, profilometry, interferometry and scanning electron microscopy were employed.*

The silica growth was parabolic after an initial linear step. The parabolic oxidation rate constants (K_P) varied with the oxygen partial pressure indicating that oxygen diffusion controlled the oxidation process. Two different apparent activation energies were found: at low temperatures ($T \leq 1350°C$) and high pressures ($P_{O_2} > 1$ atm) close to 1 eV/at, a value which corresponds to the molecular oxygen permeation through amorphous SiO_2; at high temperatures ($T \geq 1350°C$) and low pressures ($P_{O_2} \leq 1$ atm) the partial crystallization of the silica layer must be taken into account to interpret correctly the value of the apparent activation energy (2–3 eV/at).

Die Oxidationskinetik von β-SiC, hergestellt durch chemischen Dampfniederschlag (CVD) in trockenem Sauerstoff (3×10^{-2}–80 atm), wurde für einen Temperaturbereich von 1200 bis 1550°C untersucht. In situ Untersuchungen der Siliziumoxidschichtdicke bei $P_{O_2} \leq 1$ erfolgte mit Hilfe von Röntgenbeugung. Bei höheren Drücken wurden Profilometrie, Interferometrie und Rasterelektronenmikroskopie eingesetzt.

Das Siliziumoxid zeigte nach einem anfänglich linearen ein parabolisches Wachstumsverhalten. Die parabolische Oxidationsratenkonstante (K_P) variiert mit dem Sauerstoffpartialdruck, was bedeutet, daß die Sauerstoffdiffusion der prozeßbestimmende Parameter ist. Es ergaben sich zwei verschiedene scheinbare Aktivierungsenergien: bei niedrigen Temperaturen ($T \leq 1350°C$) und hohen Drücken ($P_{O_2} \geq 1$ atm) ungefähr 1 eV/at, ein Wert der demjenigen beim Durchdringen von molekularem Sauerstoff durch amorphes Siliziumoxid entspricht; bei hohen Temperaturen ($T \geq 1350°C$) und niedrigen Drücken ($P_{O_2} \leq 1$ atm) muß die teilweise Kristallisation der Siliziumoxydschicht berücksichtigt werden, um den Wert für die scheinbare Aktivierungsenergie (2–3 eV/at) richtig zu interpretieren.

On a étudié la cinétique d'oxydation du SiC β préparé par déposition en phase gazeuse sous oxygène sec (3×10^{-2}–80 atm), dans la gamme de températures 1200–1550°C. Pour $P_{O_2} \leq 1$ atm, nous avons mesuré l'épaisseur de la couche de silice par diffraction de rayons X in situ. *Pour des pressions supérieures, nous avons utilisé la profilométrie, l'interférométrie et la microscopie à balayage.*

La croissance de la silice est parabolique après un départ linéaire. Les constantes de la cinétique parabolique d'oxydation (K_P) varient avec la pression partielle d'oxygène indiquant que le processus d'oxydation est contrôlé par la diffusion de l'oxygène. Nous avons trouvé deux énergies d'activation différentes: à basse température ($T \leq 1350°C$) et pression élevée ($P_{O_2} \geq 1$ atm), elle approche 1 eV/at, valeur qui correspond à l'infiltration d'oxygène moléculaire dans SiO_2 amorphe; à haute température ($T \geq 1350°C$) et pression faible ($P_{O_2} \leq 1$ atm), il faut tenir compte de la cristallisation partielle de la couche de silice pour pouvoir interpréter la valeur de l'énergie d'activation apparente (2–3 eV/at).

1 Introduction

Like most of silicon-containing ceramic materials, SiC has a good oxidation resistance at high temperatures due to the formation of a coherent

Journal of the European Ceramic Society 0955-2219/94/$7.00 © 1994 Elsevier Science Limited, England. Printed in Great Britain

layer of silicon dioxide which protects SiC against further oxidation. Applications involving the use of SiC as a high temperature structural material, for instance in the space industry as reentry protective shields, have induced many studies in this area over the last two decades.

Moreover, SiC is also an attractive material for electronic devices because of its large band gap (2·3 for β-SiC) and high electric breakdown field (5×10^{-6} V cm^{-1}). In this area, the thermally formed SiO_2 layers on the SiC surface during oxidation are used as masks during the doping process, as passivation layers for p–n junctions or as gate dielectrics for metal oxide semiconductor (MOS) devices.

Oxidation kinetics can generally be described using the linear-parabolic model of Deal & Grove.[1] This model was developed for Si oxidation to explain the linear and parabolic dependencies of the oxide layer growth with time. This model implies that the initial stage of oxidation is reaction-rate limited and linear, but becomes parabolic as the diffusion of oxidants through the oxide becomes the rate-limiting factor. In the case of Si the reported activation energies for the linear regime correspond to the Si–Si bond energy (1·9 eV/at), in the parabolic regime activation energies[2,3] are in agreement with the energy required for molecular oxygen permeation in fused silica.[4]

The oxidation of silicon carbide, despite the numerous studies reported on it, is not as well understood, probably because of the use of many different forms of SiC: powder,[5] sintered or hot-pressed,[2,6–9] single crystal[10–13] polycrystalline CVD β-SiC.[14] Another complexity with regard to SiC arises from the presence of carbon.

Some authors[11,12] have found a linear–parabolic law, whilst others[2,10] only a simple parabolic one. In the parabolic regime many authors, in analogy with Si oxidation, suggest that the rate-controlling process is the molecular oxygen diffusion, whereas others assume that the scale growth is due to the diffusion of oxygen or silicon ions, others suggest that the outward diffusion of CO or SiO could influence the layer growth.

Costello & Tressler[13] and Zheng *et al.*[10,15] who studied the oxidation of SiC single crystals, have proposed that the mechanisms responsible for SiC oxidation were parallel transport of oxidants through the growing oxide via molecular and ionic oxygen. Molecular oxygen is the dominant permeating species at low temperatures and ionic oxygen becomes more important at high temperatures.

A scatter of papers on the nature of the silica layer also exists in the literature data and the crystalline ratio was not generally taken into account, although the oxygen diffusion coefficients through amorphous silica and through cristobalite are different at high temperatures.[16]

This paper presents results of a study of the oxidation behavior of CVD β-SiC layers in dry oxygen at 1200–1500°C under different oxygen partial pressures (P_{O_2} = 0·03, 0·22, 1, 20 and 80 atm.). Kinetics of silicon dioxide growth was determined *in situ* from quantitative high-temperature X-ray diffractometry. The purpose of the study was to determine which processes define the rate-limiting step of oxidation and to study the influence of partial crystallization during the oxidation process.

2 Experimental Procedure

2.1 Materials

The SiC samples were obtained by LPCVD (low pressure chemical vapor deposition) on to ceramic resistors made of conventional *crusilite* (90 × 8 × 2 mm^3) in order to avoid cracking produced by thermal expansion.

The CVD depositions were performed inside a cold wall reactor where the substrate was electrically heated. The reactive gases were supplied perpendicular to the substrate surface.

The reactor is associated with an X-ray diffractometer including a position sensitive detector allowing detection over a 12 degrees range.[17]

The CVD layer thickness was about 40 μm, which was large enough to prevent any impurity diffusion from the substrate to the SiC surface during the oxidation runs.

SiC was deposited using a mixture of tetramethylsilane and H_2 as gas source. The substrate was heated by transmitting an electric current. The detailed procedures of the sample preparation are explained elsewhere.[18]

The obtained CVD SiC was crystalline with the zincblende structure (β type), oriented over the (111) diffraction plane.

Before oxidation all samples were polished with diamond paste to 1 μm and ultrasonically cleaned in acetone.

2.2 Oxidation experiments

The oxidations at $P_{O_2} \leq 1$ atm were performed inside the X-ray diffraction chamber mentioned in Section 2.1. Three series of oxidations were performed varying the oxygen partial pressure: 1 atm, 150 Torr (air) and 20 Torr (O_2 mixed with He), in the temperature range 1200–1550°C. The oxidizing gas was previously dried by passing through $MgCl_2$ and P_2O_5 absorbers. Temperature was measured by optical pyrometry, taking into account the emissivity corrections[19] and the absorption through a glass window. The oxidation times were approximately 1400 min.

Kinetics were deduced from in-situ thickness versus time measurements of the silicon dioxide layer growing over SiC by mean of quantitative X-ray diffractometry. In situ X ray analysis was performed either in the Bragg–Brentano geometry for $P_{O_2} = 1$ atm or at low incidence ($\theta_i = 4°$) for lower P_{O_2} because of the slow oxidation rate in these conditions.

When a layer grows on a crystalline substrate the diffraction line intensity of the substrate decreases due to absorption according to an exponential law:[20]

$$I = I_0 \exp(-Ke) \quad (1)$$

where I is the X ray beam intensity absorbed through a layer of thickness e, I_0 is the intensity of non absorbed X ray beam and K is a coefficient including the mass absorption factor (μ/ρ) and the specific mass, ρ.

If the substrate is large enough, the thickness $e(t)$ can be simply expressed as:[21]

$$e(t) = \frac{\sin\theta}{2\mu_{ox}} \ln \frac{I_F(t)}{I_F^{\circ}(t=0)} \quad (2)$$

where θ is the Bragg angle of the analyzed (hkl) reflections, $I_F^{\circ}(t=0)$ the intensity of the SiC reflection before oxidation and $I_F(t)$ the intensity of the SiC reflection at time t. So knowing $I_F^{\circ}(t=0)$ and $I_F(t)$ the thickness of the growing layer can be determined as a function time.

Nevertheless, this expression does not work satisfactorily in case of thin layers ($e < 5\,\mu$m) because of the too small difference between I_F and $I_F^{\circ}(t=0)$ leading to poor accuracy. Consequently the increasing (111) reflection intensity of the growing silica (β cristobalite) layer was used, leading to the following relation:[22]

$$e(t) = -\frac{\sin\theta}{2\mu_{ox}} \ln\left(1 - \frac{I_B(t)}{I_M}\right) \quad (3)$$

where $I_B(t)$ is the diffracted intensity of the silica layer ((111) β cristobalite at high temperature) at time t, and I_M is the threshold intensity corresponding to a thickness which is larger than the total X ray absorption limit.

I_M could not be calculated here because the SiO_2 thickness never reached the total absorption limit, then an indirect procedure was applied. At the end of oxidation the final thickness e_f was estimated from eqn (2) and validated with other methods, such as profilometry or scanning microscopy, and associated with the corresponding final value of $I_B(t) = I_f$. Replacing $e(t)$ and $I_B(t)$ by known values e_f and I_f, I_M can be determined, leading to the following expression for $e(t)$:

$$e(t) = -\frac{\sin\theta}{2\mu_{ox}} \ln\left\{1 - \left[1 - \exp\left(-\frac{2\mu_{ox}e_f}{\sin\theta}\right)\right]\frac{I_B(t)}{I_f}\right\} \quad (4)$$

For low P_{O_2} oxidations, SiO_2 thicknesses of less than about 500 Å have to be determined, so that a low angle X ray incidence configuration is required to increase the X-ray path length into silica and so increasing X ray absorption. Then $e(t)$ can be calculated from the following expression using the increase of the (111) β cristobalite line:[22]

$$e(t) = -\frac{\sin\theta_i \sin(2\theta_B - \theta_i)}{(\sin\theta_i + \sin(2\theta_B - \theta_i))\mu_{ox}} \ln\left\{1 - \left[1 - \exp\left(-\frac{(\sin\theta_i + \sin(2\theta_B - \theta_i))\mu_{ox}}{\sin\theta_i \sin(2\theta_B - \theta_i)} e_f\right)\right]\frac{I_B(t)}{I_f}\right\} \quad (5)$$

In addition, X ray diffraction was used to estimate the crystal/amorphous ratio as a function of time and temperature, either from known standard mixtures or by separation of the amorphous and crystal contributions to the diffraction pattern.[22]

Oxidations were also performed at high oxygen pressures in a specially designed furnace working up to 1400°C and 200 atm. It consists essentially of two parts: (i) a stainless steel water cooled vessel, high pressure resistant, contains the heating element made of molybdenum coil on to a 10 cm diameter alumina cylinder. This part works in an inert gas atmosphere. The temperature is controlled by the means of a Pt 10% RhPt thermocouple set at the middle of the resistor. (ii) Inside this alumina cylinder, an alumina tube closed at one end contains the sample. A different gas (inert, oxidizing or reducing) can be introduced into this volume at equipressure with the outside. A 6% RhPt 40% RhPt thermocouple is set close to the sample for temperature measurements.

Experiments were performed at 1000, 1200 and 1360°C for two different oxygen pressures: 20 and 80 atm. As it is not possible to use the in situ X ray diffraction technique in these experiments, the thickness was determined at room temperature after the oxidation run by etching a step in the oxide and measuring its height with a stylus profilometer and scanning microscopy. Oxidation times were 90, 180, 270 and 360 min.

3 Experimental Results

3.1 Growth kinetics

Kinetic curves obtained by in-situ X ray diffraction are shown in Fig. 1. They exhibit a parabolic oxidation process after an initial linear growth, and therefore the data have been analyzed using the Deal & Grove model,[1] where the oxide thickness, X, is expressed as a function of time t, by the equation

$$\frac{X^2}{K_P} + \frac{X}{K_l} = t + \tau \quad (6)$$

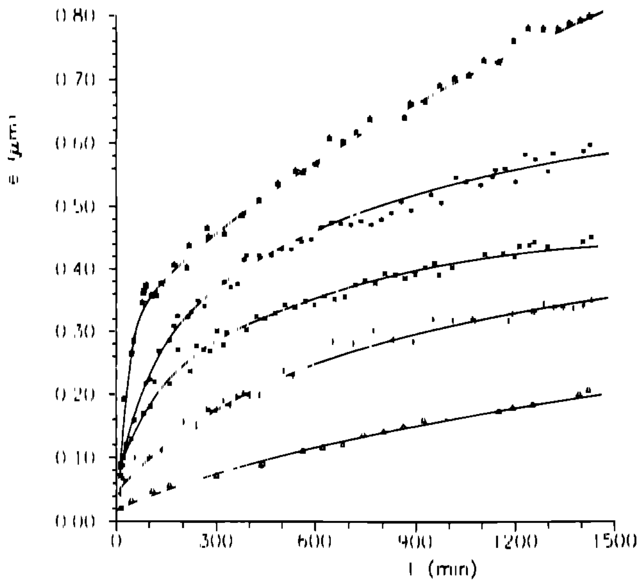

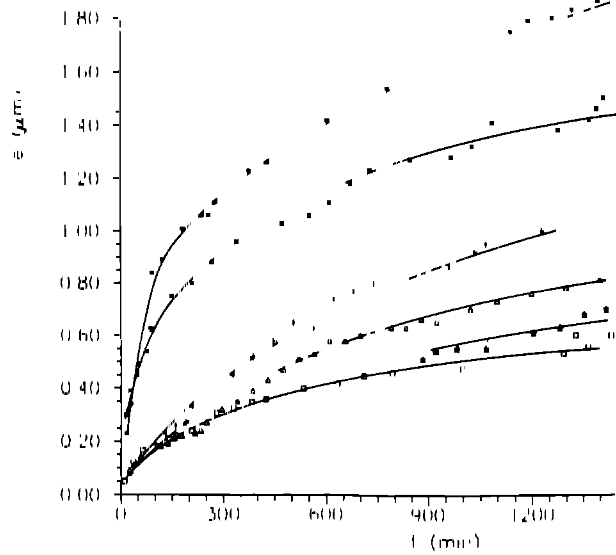

Fig. 1. Oxide thickness versus oxidation time plot for the oxidation of CVD β SiC at different oxygen partial pressures (a) P_{O_2} = 0.03 atm, T = 1310°C (△) 1360°C (+), 1420°C (•), 1475°C (∗), 1545°C (★). (b) P_{O_2} = 1 atm, T = 1200°C (□), 1250°C (☆), 1310°C (△), 1360°C (+), 1420°C (•), 1475°C (∗)

where K_l and K_p are the linear and parabolic rate constants, and τ is a time constant which accounts for an initially rapid oxidation period that is not expressed by linear or parabolic kinetics

For small times a simplified linear equation can be used

$$X = K_L(t + \tau) \tag{7}$$

while the second stage has been analyzed using eqn (6).

The curves corresponding to the high pressure experiments have been analyzed with a simple parabolic law, because not enough points were obtained to deduce a linear constant during the first minutes (Fig. 2).

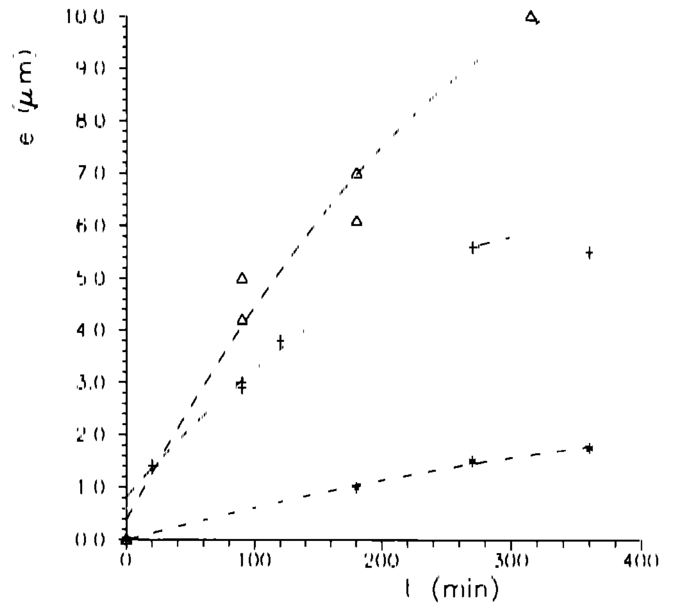

Fig. 2. Oxide thickness versus oxidation time for the oxidation of CVD β SiC at the oxygen partial pressure of 80 atm T = 1000°C (∗) 1200°C (+), 1360°C (△).

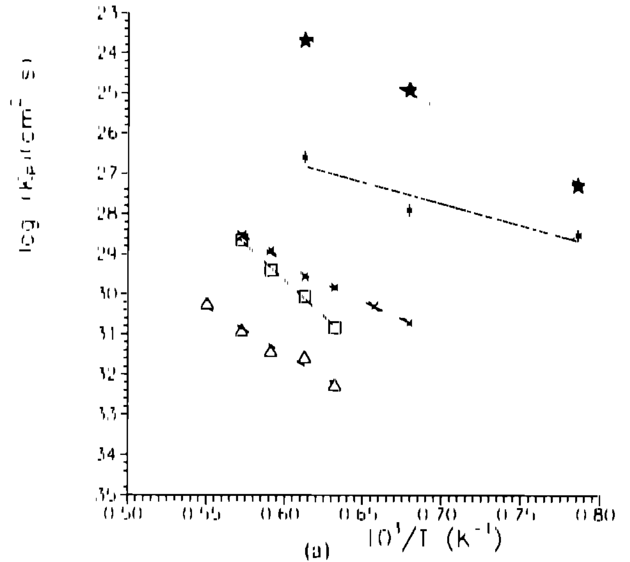

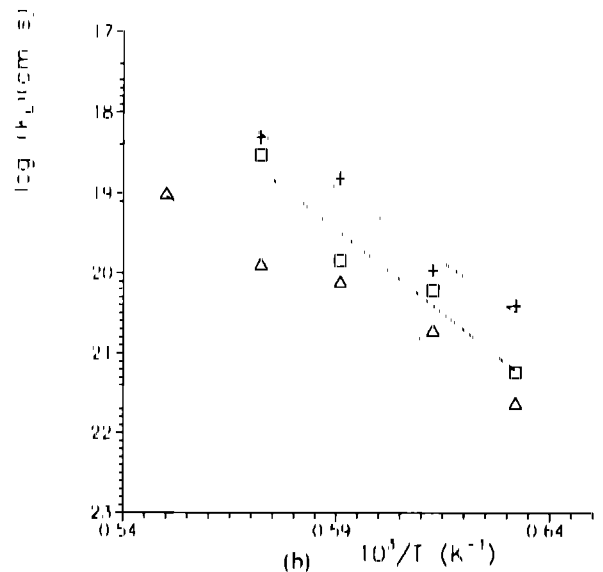

Fig. 3. Arrhenius plot of rate constants for oxidation of CVD β SiC. (a) linear rate constant; P_{O_2} = 0.031 atm (△), 0.22 atm (□), 1 atm (•) 20 atm (∗), 80 atm (★), (b) parabolic rate constant; P_{O_2} = 0.03 atm (△), 0.22 atm (□), 1 atm (+)

Table 1. Linear and parabolic rate constants for the oxidation of CVD β SiC at several dry oxygen pressures

T (°C)	$(K_L, K_P) \times 10^{-13}$ (cm^2/s)				
	P_O (atm)				
	80	20	1	0.22	0.031
1000	$K_P = 14$	$K_P = 4.0$		–	
1200	$K_P = 150$	$K_P = 7.5$	$K_P = 0.42$		–
1250			$K_P = 0.68$	–	
1310		–	$K_P = 1.1$	$K_P = 0.40$	$K_P = 0.096$
	–	–	$K_L = 1.3$	$K_L = 0.60$	$K_L = 0.40$
1360	$K_P = 520$	$K_P = 28$	$K_P = 1.45$	$K_P = 0.87$	$K_P = 0.19$
		–	$K_L = 2.1$	$K_L = 1.65$	$K_L = 1$
1420	–		$K_P = 2.8$	$K_P = 1.7$	$K_P = 0.22$
		–	$K_L = 6.7$	$K_L = 2.4$	$K_L = 1.8$
1475		–	$K_P = 4.0$	$K_P = 3.6$	$K_P = 0.37$
	–		$K_L = 11.1$	$K_L = 8.95$	$K_L = 2.3$
1545		–	–	–	$K_P = 0.72$
			–		$K_L = 5.5$

Table 2. Activation energies for the oxidation of CVD β SiC at several dry oxygen pressures

P_O (atm)	ΔE(eV) (linear regime)	ΔE(eV) (parabolic regime)
0.031	2.6	2.0
0.22	3.6	3.1
1	3.2	1.60 ($T \leq 1350$ °C), 2.2 ($T \geq 1350$ °C)
20		0.95
80	–	1.8

Table 1 shows the values of the linear and parabolic rate constants for the different temperatures and pressures.

The apparent activation energies for oxidation in the linear and parabolic regime were determined from the ln (K_P, K_L) versus $1/T$ relation. Figure 3 shows this plot and the values are listed in Table 2.

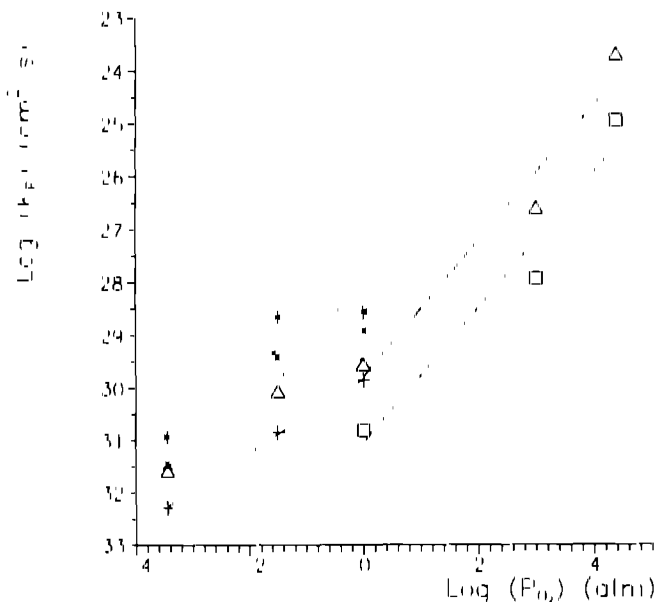

Fig. 4. Oxygen partial pressure (P_{O_2}) dependence of the parabolic rate constant (K_P).

Figure 4 shows the relationship between the oxygen partial pressure (P_{O_2}) and the parabolic rate constant K_P at the different temperatures. Despite the poor accuracy a general trend can be determined showing that for $P_{O_2} < 1$ atm K_P is proportional to the first power of the oxygen partial pressure ($n \simeq 1$), whilst at $P_{O_2} > 1$ atm this dependence is lowered to $n \simeq 0.7$.

3.2 Morphology of the oxidation layers

The oxide scale generally consisted of a mixture of amorphous and crystalline silica. As shown in Fig. 5, the small radially crystallized disks, consisting of cristobalite as characterized from X-ray diffraction patterns, are dispersed in an amorphous phase

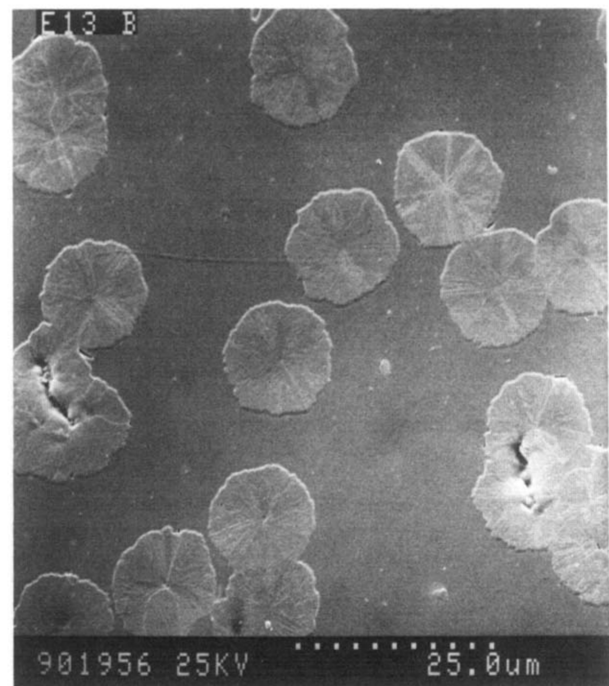

Fig. 5. Scanning electron micrograph of spherulites on SiC for 1420 min at 1250 °C.

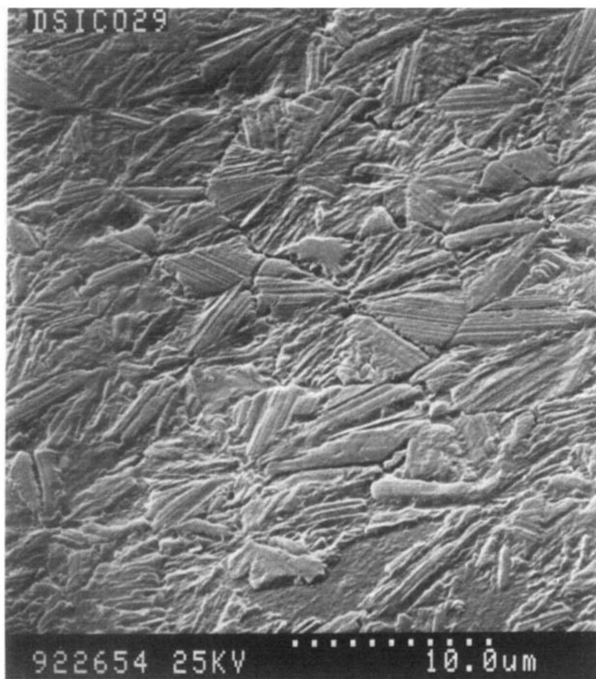

Fig. 6. Scanning electron micrograph of spherulitic features in the oxide film on CVD β SiC oxidized at 1540 C

When the temperature increases, the crystalline phase increases also, leading to a higher density. At high temperatures the radii are limited by impingement. Figure 6 shows the formation of a continuous layer of spherulites at $T = 1540$ C. Delineation of the spherulitic crystals is achieved by the preferential

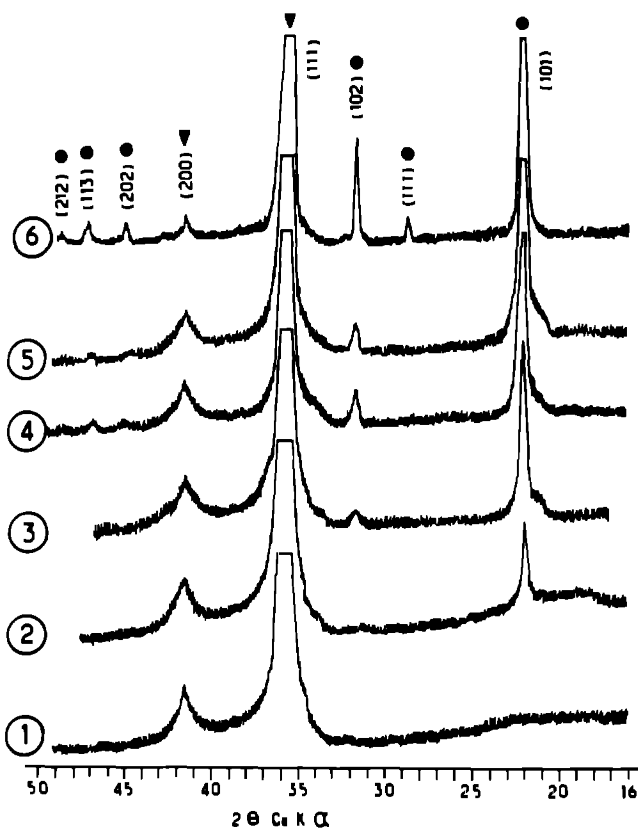

Fig. 7. X ray diffraction pattern showing the evolution of cristobalite at the different temperatures after cooling, P_{O_2} = 1 atm. All oxidation times were approximately 1400 min. ●, Cristobalite; ▼, β SiC

Table 3. Crystal/amorphous ratio in the oxide scale for specimens oxidized at different temperatures and oxygen pressures

P_{O_2} (atm)	T (C)	% crystallinity
	1 310	65 ± 10
	1 360	75 ± 10
0.031	1 420	85 ± 10
	1 475	95 ± 10
	1 545	100 ± 10
	1 310	15 ± 10
0.22	1 360	20 ± 10
	1 420	30 ± 10
	1 475	100 ± 10
	1 200	15 ± 10
	1 250	50 ± 15
1	1 310	65 ± 15
	1 360	75 ± 15
	1 420	85 ± 10
	1 475	95 ± 10

removal of the amorphous phase resulting from differences in the etching rate of the oxide phases in the HF etch.

Figure 7 shows the evolution of the α-cristobalite (101) line with oxidation temperature due to either the greater oxide thickness and the superior degree of crystallization.

The crystal/amorphous ratio determined from the scanning micrographs is in good agreement with the results obtained from X-ray diffraction analysis. Table 3 shows the crystal/amorphous ratios for the different experimental conditions.

For high pressure oxidations (20–80 atm) X-ray diffraction patterns showed the presence of small amounts of trydimite besides cristobalite.

4 Discussion

The X ray diffraction technique used here allowed in-situ determinations of the amorphous and crystalline contribution to the X ray signal. In fact, after an initial transient period, the crystal/amorphous ratio did not show any significant variation within the accuracy of this kind of measurement, which is close to 15%.

The reason why a steady crystalline/amorphous ratio is attained in the first stage of oxidation can be understood by considering the crystallization kinetic data of bulk silica materials. Verduch[23] suggested that the formation of cristobalite involves three processes as a function of time: firstly the nucleation, which depends strongly on temperature; secondly, the growth of a cristobalite like type of structure involving short range movements of particles, and thirdly, a much slower process which corresponds to a state of apparent equilibrium in which the imperfect nature of the cristobalite initially formed transforms into a cristobalite with a higher degree

of order. Ramachandran *et al.*[24] also found a similar behavior for samples heated to 1600°C.

It seems reasonable to think that defects present on the polycrystalline β-SiC surface, such as multigrain junctions, lower the energy necessary to overcome the nucleation barrier and therefore produce faster nucleation and an enhancement of crystallization.

Changes in surface defect concentrations may explain the differences between polycrystalline SiC, which induces crystallization of the oxide scale[7,12,25] and SiC single crystals over which amorphous silica can be thermally grown up to ≥1400°C.[10]

The dependence of the degree of crystallization on the surface defect concentration is evident from Table 3. Samples oxidized in air have a significant lower crystallinity induced by the better surface quality. Later on the influence of crystallinity on the oxidation process will be discussed.

The spherulites shown in Fig. 5 have approximately the same diameter, suggesting a cristobalite growth process involving only pre-existing nuclei.

The kinetic curves of dry oxidation at different P_{O_2} and temperatures are shown in Figs 1 and 2. The linear rate constants (K_L) are plotted as a function of the reciprocal of the absolute temperature in Fig. 3. The activation energies of the linear rate constants for each pressure were determined from the slope of each line. It can be seen that the temperature dependence is quite similar for each pressure, with the activation energies of the linear rate constants for P_{O_2} = 0.03, 0.22 and 1 atm having values of 2.6, 3.6 and 3.2 eV/at, respectively. These activation energies are related to the initial reaction-rate limited regime of oxidation and correspond to the 3 eV/at required to break a Si–C bond.[12,26]

The activation energy of the parabolic regime has to be related to a diffusional process. Some recent experimental data about the parabolic rate constants of SiC oxidation for different types of the material are summarized in Table 4. Surprisingly, there are no significant differences between the polycrystalline samples: stoichiometric CVD β-SiC, sintered α-SiC or hot pressed SiC, which means that the presence of additives, such as 1% B in the sintered α-SiC, does not significantly affect the growth of the oxide layer. The major difference between sintered α-SiC and CVD β-SiC is that gas bubbles form in the silica scales on sintered α-SiC at much lower temperatures owing to the formation of boron hydroxide.[27] Single crystals (0001 Si face) exhibit lower parabolic rate constants.

More specific comments are not possible because there are insufficient data about important parameters like the crystallinity degree of the oxide scale, the presence of impurities or the surface state.

The dependence of the oxidation rate on the

Table 4. Comparison between parabolic rate constants obtained for different types of SiC

Material	$K_p \times 10^{-13}$ ($cm^2\ s^{-1}$)			
	1200°C	*1300°C*	*1400°C*	*1500°C*
Sintered α-SiC[18]	0.37	0.98	2.3	—
Single crystal SiC[10] (000$\bar{1}$) C face	0.29	0.50	0.96	2.0
Single crystal SiC[10] (0001) Si face	0.063	0.38	0.80	2.1
Sintered α-SiC[19]	0.4	0.65	1.20	
Single crystal α-SiC[13] (000$\bar{1}$) C face	0.47	1	1.70	3.85
Single crystal α-SiC[13] (0001) Si face	0.031	0.29	1.4	2.95
CNTD poly SiC[13]	0.57	1.25	2.3	7.5
Hot pressed SiC[13]	0.37	1.2	3.1	—
Hot pressed SiC[18]	0.49	1.1	2.2	—
CVD β-SiC[a]	0.42	0.98	2.1	5.1

[a] This work.

oxygen partial pressure (P_{O_2}) shown in Fig. 4 implies that the rate controlling process of the oxidation is due to the diffusion of oxygen in the oxide film. If oxygen diffuses in molecular form, the parabolic rate constant (K_P) varies directly with the oxygen partial pressure (P_{O_2}),[4] whereas if it diffuses in ionic form, K_P will vary as the square root of the oxygen partial pressure ($P_{O_2}^{1/2}$).

Jorgensen *et al.*[28] reported the ($P_{O_2}^{1/2}$) dependence in the oxidation rate of SiC powder at 1573 K to 1829 K and indicated that the rate controlling process was the diffusion of oxygen ions. Costello & Tressler[13] reported that the oxidation mechanism would change above 1673 K. For lower temperatures they showed that the oxidation is controlled by molecular oxygen diffusion through the SiO_2 film and predicted the diffusion of oxygen ions as the rate controlling factor and the ($P_{O_2}^{1/2}$) dependence above 1673 K. Zheng *et al.*[15] confirmed the existence of parallel transport via molecular and ionic oxygen during the oxidation of SiC single crystals. They observed a decrease in the oxygen pressure dependence ($K_P \propto P_{O_2}^n$) of the parabolic rate constant from n = 0.6 at 1200°C to n = 0.3 at 1500°C.

In this work, K_P was proportional to P_{O_2} at low temperatures ($T \leq$ 1360°C) and high pressures and to ($P_{O_2}^{n}$) for higher temperatures and lower pressures. This change in the pressure dependence, despite the uncertainty introduced by the use of only three points in some cases, suggests the presence of two different mechanisms.

Table 2 shows the apparent activation energy values corresponding to the parabolic regime. At temperatures lower than approximately 1350°C the activation energy values (1.1.6, 1.8 eV/at) are lower than the values obtained at high temperatures, $T \geq$ 1350°C (2, 2.2, 3.1 eV/at). This difference is more evident in the samples oxidized at 1 atm O_2 where

the temperature range was large enough to appreciate the activation energy changes

This change strongly suggests the presence of two oxidation mechanisms, but the activation energy values are too scattered to deduce which one is taking place. To solve this problem, the crystallinity of the SiO_2 film and the presence of short circuits (cracks) is taken into account in some cases

In an earlier paper[16] it was shown that oxygen lattice diffusion through amorphous silica was faster than through β cristobalite, with activation energies of 4.5 eV/at and around 3.5 eV/at, respectively. Thus, if ionic oxygen diffusion is the rate controlling process, the parabolic rate constant must be proportional to its diffusivity value through the oxide layer, $K_P \propto (D_O(SiO_2))$. It has been shown already that during CVD β SiC oxidation silica grows more or less crystallized, mainly depending on temperature. As the crystallinity percentage varies with temperature, the apparent K_P value obtained experimentally is in fact the average of two contributions with different weights (for the amorphous or the crystal) as a function of temperature. K_P can be expressed as

$$K_P = x K_P(\mathrm{am}) + (1 - x) K_P(\mathrm{cr}) \quad (8)$$

where x is the amorphous fraction

If K_P follows an Arrhenius relationship

$$K_P = x K_P^0(\mathrm{am}) \exp\left(-\frac{\Delta E}{kT}\right) + (1 - x) K_P^0(\mathrm{cr}) \exp\left(-\frac{\Delta E'}{kT}\right) \quad (9)$$

where ΔE and $\Delta E'$ are the activation energies corresponding to diffusion through amorphous SiO_2 and β-cristobalite, respectively

If it is considered that $\Delta E'(\mathrm{cr}) \simeq \Delta E(\mathrm{am}) + 1$ eV/at and that $D_O^0(\mathrm{cr}) \simeq 500\, D_O^0(\mathrm{am})$ with a variation of $D(\mathrm{am})/D(\mathrm{cr})$ from 10 at 1200°C to 2.5 at 1500°C,[16] then taking into account these data, the experimental K_P value can be expressed in function of the amorphous or crystalline K_P as

$$K_P = K_P^0(\mathrm{am}) \exp\left(-\frac{\Delta E(\mathrm{am})}{kT}\right) \left[x + 500(1 - x) \exp\left(\frac{\Delta E(\mathrm{am}) - \Delta E'(\mathrm{cr})}{kT}\right)\right] \quad (10)$$

$$K_P = K_P^0(\mathrm{cr}) \exp\left(-\frac{\Delta E'(\mathrm{cr})}{kT}\right) \left[(1 - x) + \frac{x}{500} \exp\left(\frac{\Delta E'(\mathrm{cr}) - \Delta E(\mathrm{am})}{kT}\right)\right] \quad (11)$$

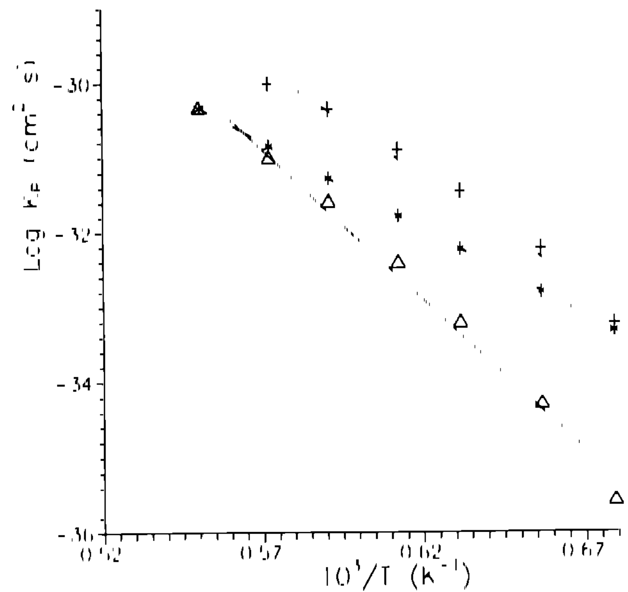

Fig. 8. Influence of partial crystallization over the apparent activation energy obtained from the K_P values, $\ast$, experimental, $\triangle$, crystal, $+$, amorphous

Figure 8 shows the plot obtained using eqns (10) and (11) for $P_{O_2} = 0.03$ atm

So, if the apparent activation energy values of 2 and 2.2 eV/at obtained at $P_{O_2} = 0.03$ and 1 atm are corrected from the crystallinity variation, values close to 3 eV/at are obtained for $K_P(\mathrm{am})$, and close to 4 eV/at for $K_P(\mathrm{cr})$, which agree better with the activation energy values found by tracer diffusion experiments, 3.4 and 4.5, respectively.[16] The higher activation energy value (3.1 eV/at) found for samples oxidized in air is in agreement with the lower crystallinity percentage of this samples.

Now let the apparent activation energy values obtained at low temperatures be considered. Values close to 1 eV/at agree well with the activation energy for the permeation of molecular oxygen through silica glass (1.2 eV/at).[4] The value of 1.8 eV/at corresponding to samples oxidized at 80 atm should be explained by the existence of pores and cracks in the crystallized samples. These short circuits induce a faster oxidation rate which cause an increase in the apparent activation energy value. As no data is available about the molecular oxygen permeation through β-cristobalite and as the six-fold rings responsible for this type of diffusion are present in both amorphous silica and β-cristobalite,[29] it is considered that molecular diffusion is not influenced by crystallization

Thus, the low temperature activation energies for the parabolic regime are close to 1 eV/at, indicating that the rate-controlling process is the molecular oxygen permeation through the silica layer. At high temperatures, the apparent activation energies correspond to processes with higher activation energies ($\simeq$ 3–4 eV/at), suggesting the existence of a process limited by ionic oxygen diffusion.

5 Conclusions

Oxidation of CVD β SiC followed parabolic kinetics after an initial linear growth.

The parabolic rate constant, K_p, increased strongly with increasing partial pressure, indicating that the rate controlling process for oxidation is the diffusion of oxygen through the SiO_2 film. Two values of the oxygen partial pressure exponent, n, were found, at $T \leq 1350°C$, $n \simeq 1$ and at $T \geq 1360°C$, $n \simeq 0.7$, suggesting the presence of two mechanisms for oxygen diffusion.

The activation energy values of around 1 eV/at at low temperatures are about the same as that of oxygen permeation through fused silica.[4] The activation energy values at high temperatures are somewhat higher, indicating an important contribution of ionic oxygen to the silica growth. In this case, the analysis of the apparent activation energy value is complex, due to the partial crystallization of the oxide layer, because lattice oxygen diffusion in amorphous SiO_2 is faster than in β-cristobalite.[16]

With the aid of the crystal/amorphous ratio determination in the silica layer, it has been shown that the apparent activation energy value can be interpreted as the mixture of two contributions with activation energies close to that of oxygen diffusion through amorphous SiO_2 (3·4 eV/at) and β cristobalite (4·5 eV/at).

A detailed kinetic analysis of the presence of molecular and ionic oxygen diffusion, also including the effect of partial crystallization, is given in a companion paper.[30]

Acknowledgement

The authors are indebted to Prof. R. W. Cahn for correction of the manuscript and for valuable discussions. J.R. and M.T.C.M. wish to acknowledge financial support from CICYT (project MAT 92/0501).

References

1 Deal, B. E. & Grove, A. S., General relationship for the thermal oxidation of silicon. *J. Appl. Phys.*, **36** (1965) 3770.
2 Costello, J. A. & Tressler, R. E., Oxidation kinetics of hot pressed and sintered α SiC. *J. Am. Ceram. Soc.*, **64**(6) (1981) 327.
3 Rosencher, E., Straboni, A., Rigo, S. & Amsel, G., An ^{18}O study of the thermal oxidation of silicon in oxygen. *Appl. Phys. Lett.*, **34** (1979) 254.
4 Norton, F. J., Permeation of gaseous oxygen through vitreous silica. *Nature*, **191**(7) (1961) 971.
5 Pampuch, R., Ptak, W., Jonas, S. & Stoch, J., Formation of ternary Si-O-C phase(s) during oxidation of SiC. *Mater. Sci. Monogr.*, **6** (1980) 435.
6 Singhal, S. C., Oxidation kinetics of hot pressed silicon carbide. *J. Mat. Sci.*, **11** (1976) 1246.
7 Zdaniewsky, W. A. & Kirchner, H. P., Effect of grain boundary oxidation on fracture toughness of SiC. *J. Am. Ceram. Soc.*, **70**(8) (1987) 548.
8 Li, J., Etudes de l'oxydation de SiC et du comportement diffusionnel de ^{13}C et de ^{29}Si implantes dans SiC. PhD thesis, Universite Paris Sud, Orsay, 1990.
9 Mitchell, T. E. & Heuer, A. H., Oxidation of non oxide ceramics. Technical report, Air Force of Scientific Research, Contract F49620-78-C-0053, 1982.
10 Zheng, Z., Tressler, R. E. & Spear, K. E., Oxidation of single crystal silicon carbide. I. Experimental study. *J. Electrochem. Soc.*, **137**(3) (1990) 854.
11 Fung, C. D. & Kopanski, J. J., Thermal oxidation of 3c silicon carbide single crystal layers on silicon. *Appl. Phys. Lett.*, **45**(7) (1984) 757.
12 Palmour, J. W., Kim, H. J. & Davis, R. F., Wet and dry oxidation of single crystal β SiC: kinetics and interface characteristics. In *Thin Films Interfaces and Phenomena*, Materials Research Society, 1985.
13 Costello, J. A. & Tressler, R. E., Oxidation kinetics of silicon carbide crystals and ceramics. I. In dry oxygen. *J. Am. Ceram. Soc.*, **69**(9) (1986) 674.
14 Narushima, T., Goto, T. & Hirai, T., High temperature passive oxidation of chemically vapor deposited silicon carbide. *J. Am. Ceram. Soc.*, **72**(8) (1989) 1386.
15 Zheng, Z., Tressler, R. E. & Spear, K. E., Oxidation of single crystal silicon carbide. II. Kinetic model. *J. Electrochem. Soc.*, **137**(3) (1990) 2812.
16 Rodriguez Viejo, J., Sibieude, F., Clavaguera Mora, M. T. & Monty, C., ^{18}O diffusion through amorphous SiO_2 and β cristobalite. *Appl. Phys. Lett.*, **63** (1993) 1906.
17 Lartigue, J. F. & Sibieude, F., Diffractometri X a haute temperature sur CVD Si_3N_4. *Rev. Int. Hautes Temp.*, **22** (1985) 71.
18 Sibieude, F. & Benezech, G., Chemical vapor deposition of SiC: an X ray diffraction study. *J. Mater. Sci.*, **23** (1989) 1632.
19 Touloukian, Y. S., *Thermal Radiative Properties, Coatings*, Vol. 9. IFI Plenum, 1985.
20 Guinier, A., *Theorie et Technique de la Radiocristallographie*. Dunod, Paris, 1964.
21 Fatu, D., Etude de la cinetique d'oxydation des metaux par la methode radiocristallographique. *Mater. Chem.*, **6** (1981) 55.
22 Rodriguez Viejo, J., Contribucion al estudio de la cinetica de oxidacion de CVD β SiC y analisis del comportamiento difusional del oxigeno SiO$_2$. PhD thesis, Universidad Autonoma de Barcelona, Spain, 1992.
23 Verduch, A. G., Kinetics of cristobalite formation from silicic acid. *J. Am. Ceram. Soc.*, **41** (1958) 427.
24 Ramachandran, B. E., Bala Singh, C. & Pai, B. C., Studies on the crystallization behaviour of high silica materials. *Mater. Sci. Eng.*, **67** (1984) L5.
25 Ogbuji, L. U., Oxidation of polycrystalline silicon carbide. *Ceram. Int.*, **12** (1986) 173.
26 Pauling, L., *The Nature of the Chemical Bond and the Structure of Molecules and Crystals*. Cornell University, NY, 1960.
27 Fergus, J. W. & Worrell, W. L., In *Corrosion and Corrosive Degradation of Ceramics*, ed. R. E. Tressler & M. McNallan. American Ceramic Society, Inc.
28 Jorgensen, P. J., Wadsworth, M. E. & Cutler, I. B., Effects of oxygen partial pressure on the oxidation of silicon carbide. *J. Am. Ceram. Soc.*, **44**(6) (1961) 258.
29 Galeener, F. L., Planar rings in vitreous silica. *J. Non Cryst. Solids*, **49** (1982) 53.
30 Rodriguez Viejo, J., Sibieude, F. & Clavaguera Mora, M. T., High temperature oxidation of CVD β SiC. Part II. Relation between oxygen diffusion coefficients and parabolic rate constants. *J. Eur. Ceram. Soc.*, **13** (1994) 177–84.